

# We are IntechOpen, the world's leading publisher of Open Access books Built by scientists, for scientists

6,900

Open access books available

186,000

International authors and editors

200M

Downloads

Our authors are among the

154

Countries delivered to

TOP 1%

most cited scientists

12.2%

Contributors from top 500 universities



WEB OF SCIENCE™

Selection of our books indexed in the Book Citation Index  
in Web of Science™ Core Collection (BKCI)

Interested in publishing with us?  
Contact [book.department@intechopen.com](mailto:book.department@intechopen.com)

Numbers displayed above are based on latest data collected.  
For more information visit [www.intechopen.com](http://www.intechopen.com)



# Electrodynamics of High Pinning Superconductors

Klimenko E.Yu.

*National Research Nuclear University "MEPhI"*

*Russian Federation*

## 1. Introduction

High pinning superconductors (HPSC) hold much promise for power engineering. There are some annoying consequences of up-to-date unequal state of these materials electrodynamic. The main one is for lack of superconducting winding engineering environment. Applied superconductivity is still a field of empirical activity. There are two ways for a reliable design developing, either using of steady state stabilized conductor with a lot of normal metal, or protracted trial-and-error manufacturing of full-scale model windings. Both ways are too expensive. In the narrow sense, new approaches are called for effective computation of real conductor stability, loss, etc. Probably in the more wide sense, putting the fundamentals in order will provide more stability to the whole applied superconductivity for opposition from new wasteful initiatives. The state of HPSC physics gives another cause for concerning. Now it is a vast collection of incoherent effects and several options of mesoscopic models for each one. The analysis of the situation has uncovered the following probable causes of the modern state of the electrodynamic: 1. the most popular constitutive law so called thermal activation model [Anderson 1962], is not only inconvenient but most likely unequal; 2 a good deal of discovered effects is conditioned by incorrect data processing.

A detailed examination [Klimenko et al., 2005] had shown that in fact the thermal activation hypothesis had neither grounds nor verifications. However, taking into account the fabulous popularity of the hypothesis we considered necessary to revise all the points from the beginning [Klimenko et al., 2005].

This paper contains an alternative constitutive law and reasoning in its favour, general setting up the problem of quasisteady HPSC electrodynamic, and discussion of some features of HPSC which must be kept in mind during experiment setting up and data processing.

## 2. HPSC constitutive law (Nb-Ti)

There were several reasons for selecting a niobium-titanium as the material for constitutive law revising. It is analogous to niobium-zirconium wires widely used in basic experiments favouring establishment of the thermal activation model. However, this is not the only ground for this choice: we believe niobium-titanium wire and foil to be the most suitable materials for studying the transition characteristics of superconductors with high pinning as well as the problems of their electrodynamic. The high level of commercial technology of niobium-titanium alloys provides relatively homogeneous materials exhibiting uniform

properties along the wire length and the foil area. The niobium–titanium conductors are convenient for pinning anisotropy studying. Sufficiently high anisotropic pinning is not complicated with critical field anisotropy. No other commercially available material offers these advantages. These advantages make it possible to study the general laws of electrodynamics in technical superconductors [Klimenko et al., 1997], which are almost not masked by specific features of particular samples. Experiments with niobium–titanium wires are not complicated by brittleness and high sensitivity to straining; those are typical features of intermetallic compounds and HTSC. On the other hand, niobium–titanium wires are by no means a simple material. These wires were displaced from the focus of research, not even having been exhaustively studied. Later, it was found that niobium–titanium alloys are two-component (as manifested by a difference in the critical fields of the grain body and boundaries [Klimenko et al., 2001a]) and are characterized by anisotropic pinning in the cross section of a wire [Klimenko et al., 2001b].

We used a commercial monofilament copper coated Nb-50wt%Ti wire 0.15 mm in diameter. Superconducting core diameter was 0.12 mm. Several dozens of voltage-current curves were recorded in magnetic field range from zero up to  $B_{c2}$  [Klimenko et al., 2005]. The curves were converted into ohm-ampere ones. The latter were linear in semi-logarithmic scale at several

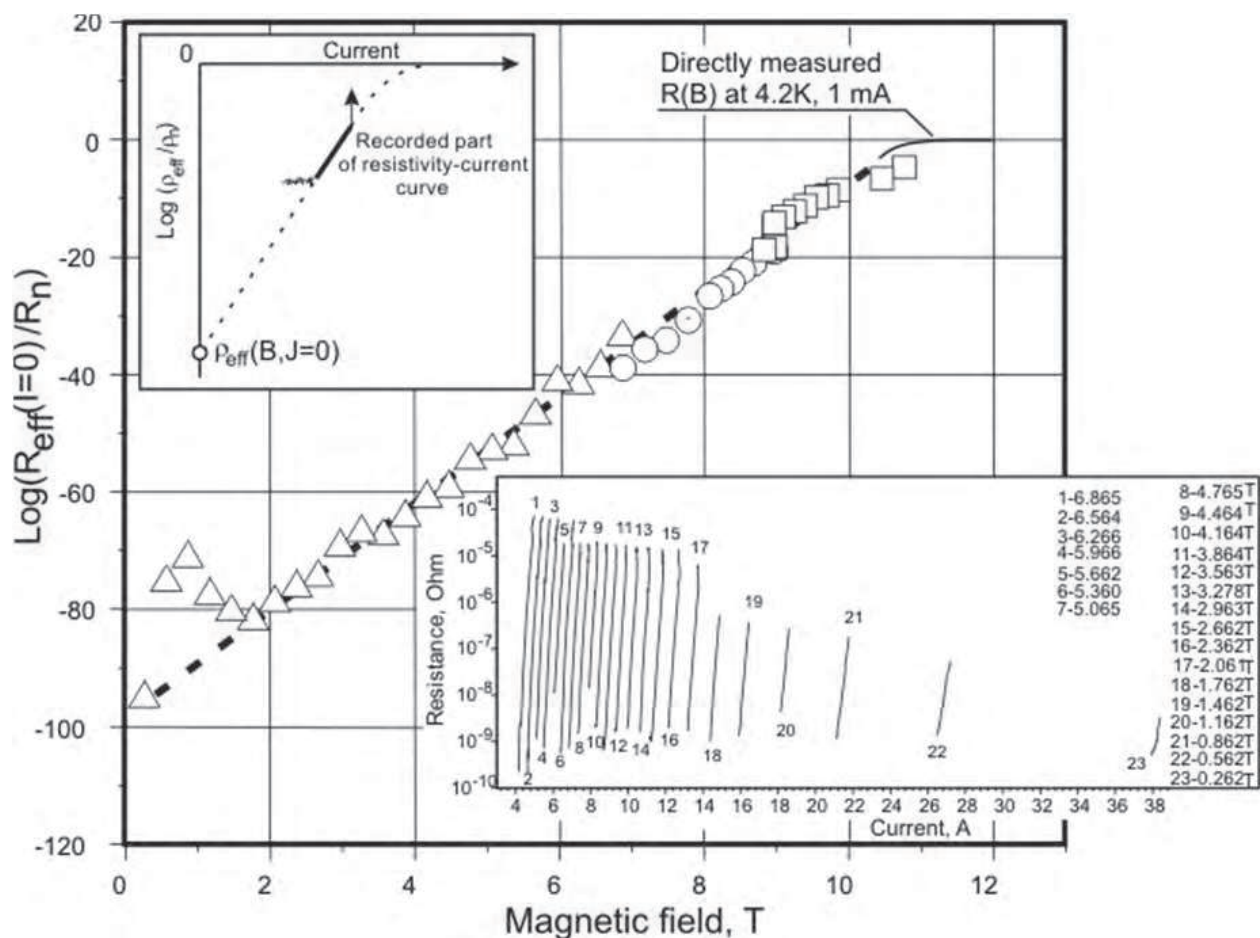


Fig. 1. Dependence of reduced resistivity of Nb-Ti wire on magnetic field at zero current [11]. The resistivity was obtained by the extrapolation of ohm-ampere curves to zero current. Some of the used ohm-ampere curves are shown on a panel. Another panel illustrates the extrapolation procedure.

orders of resistance values. There were two reasons to use just ohm-ampere curves. Firstly, a finite value of resistance being obtained by the curve extrapolation to zero current (Fig.1) was quite natural contrary to a finite voltage value at zero current. The later self-contradiction of thermal activation model is avoidable by no workarounds [Ketterson&Song]. Secondly, this approach corresponded to usual way of critical values determination, say,  $T_c$  and  $B_{c2}$ .

The experimental results were compared with a simplest constitutive law proposed thirty years ago [Dorofeev et al., 1980]:

$$\sigma(T, B, j) = \sigma_n \left\{ 1 + \exp \left[ \left( -1 + \frac{T}{T_c} + \frac{|B|}{B_{c2}} + \frac{|j|}{j_c} \right) \frac{1}{\delta} \right] \right\} \quad (1)$$

The law was derived from assumption that a critical surface ( $\frac{T}{T_c} + \frac{B}{B_{c2}} + \frac{j}{j_c} = 1$ ) in its traditional form should be replaced with a smooth transition layer. The comparison is not complicated because expression (1) contains only one fitting parameter: critical current corresponding to effective resistivity equal to a half of normal one at zero temperature and zero magnetic field. In the strict sense,  $T_c$  and  $B_{c2}$  are also fitting parameters, but they must be closely alligned to the critical values measured at small current. Fig.2 shows that this critical current value is a good constant, as well as parameter  $\delta$  describing transition width. Corresponding to another measurement series [Dorofeev et al., 1979] Fig.3 shows rather a vast tablelands of the parameters in dependence on temperature and magnetic field. Their rise at low magnetic field governs with pinning anisotropy. It will be discussed in part 5 of the paper.

It follows from (1) that nothing as “true critical current” exists. More likely a certain insignificant seed resistivity exists at zero temperature and magnetic fields. The resistivity increases exponentially with raising any parameter  $T$ ,  $B$  or  $j$ . Fig.1 is a kind of this conception confirming. However, the extremely low resistivity is more likely statistics of local resistive barriers than the homogeneous property. Anybody will be wrong calculating, for example, skin depth by using this resistivity. This value may not be less than  $\lambda$  (length of field penetration depth into superconductor).

An isotropic HPSC is a media which conductivity depends on magnetic field direction relative to current. In this case the conductivity must be a tensor. Current density and electric field are related through the material equation:

$$j_\alpha = \sigma_{\alpha\beta} E_\beta \quad (2)$$

Where  $\sigma_{\alpha\beta}$  just is the electrical conductivity tensor.

According to the general principles, the electrical conductivity tensor for high pinning superconductors in magnetic field obeys the condition

$$\sigma_{\alpha\beta}(\mathbf{B}) = \sigma_{\beta\alpha}(-\mathbf{B}) \quad (3)$$

The part of the conductivity tensor odd with respect to magnetic field is antisymmetric with respect to transposition of indices and determines the physical phenomena such as Hall Effect etc. This part does not contribute to the heat generation and is small in superconductors. Therefore, we restrict ourselves only with the symmetric part of this tensor. For isotropic superconductors in magnetic field the symmetric part may be presented in the form

$$\sigma_{\alpha\beta} = \sigma_t(\delta_{\alpha\beta} - b_\alpha b_\beta) + \sigma_l b_\alpha b_\beta \quad (4)$$

Here  $\delta_{\alpha\beta}$  is Kronecker delta and  $b$  is the unit vector along the magnetic field  $B$ . In the normal state the electrical conductivity is isotropic,  $\sigma_t = \sigma_l = \sigma_n$ , and  $j = \sigma_n E$ . The first term in the right-hand side of (4) refers to the dissipative motion of vortices under the action of Lorentz force. The longitudinal part  $\sigma_l$  in (4) is related to the dissipation processes induced when the current flows along magnetic field. Although the longitudinal conductivity  $\sigma_l$  is well-established, its influence, as well as the tensor character of HPSC electrical conductivity, is commonly neglected in the applied researches. Such approximation holds only when current and magnetic field are mutually perpendicular. That is not the case, for example, in twisted multifilament wires.

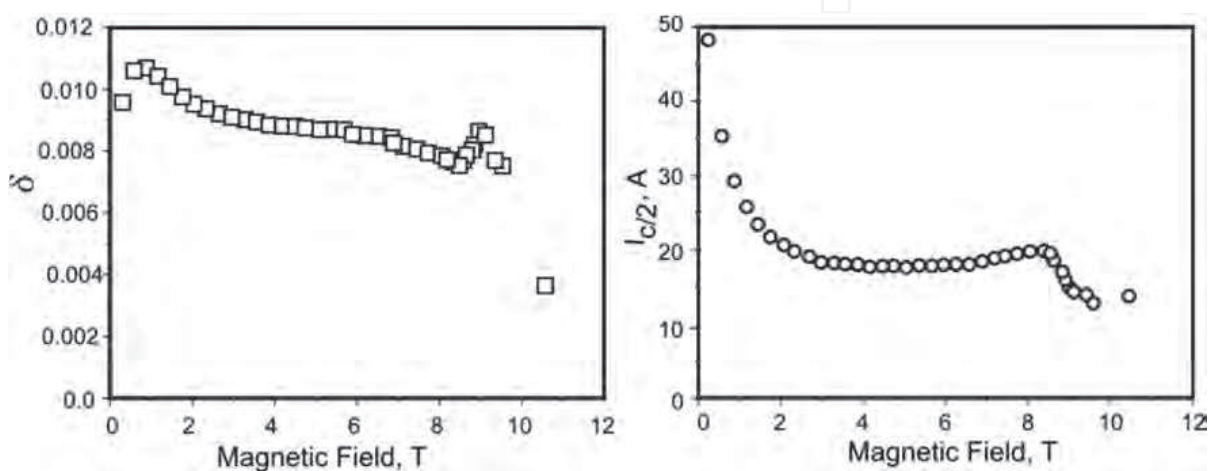


Fig. 2. The parameters describing Nb-Ti wire transition are surprisingly stable

In the critical state model, it is assumed that the transition from the superconducting state to normal one occurs when physical parameters attain the critical surface

$$K(T, |B|, |j|) = 0 \quad (5)$$

where  $|B|$  and  $|j|$  are modules of a vector. Due to intrinsic textural inhomogeneity of HPSC the actually observed transition to resistive state is smoothed at the vicinity of critical state. The tensor approach requires generalising of (1) for the transverse and longitudinal parts of electrical conductivity in superconductors:

$$\sigma_t = \sigma_n \left[ 1 + \exp\left(\frac{K_t}{\delta}\right) \right] \quad (6)$$

$$K_t = 1 - \frac{T}{T_c} - \frac{|B|}{B_{c2}} - \frac{|j|}{j_{c/2}^t} \quad (7)$$

$$j_{t\alpha} = (\delta_{\alpha\beta} - b_\alpha b_\beta) j_\beta \quad (8)$$

here  $\delta_{\alpha\beta} = \begin{cases} 1, & \alpha = \beta \\ 0, & \alpha \neq \beta \end{cases}$  is Kronecker delta. It has nothing common with  $\delta$  in (1, 6 and 9). By analogy with (6-8) longitudinal conductivity may be written

$$\sigma_l = \sigma_n \left[ 1 + \exp\left(\frac{K_l}{\delta}\right) \right] \quad (9)$$

$$K_l = 1 - \frac{T}{T_c} - \frac{|B|}{B_{c2}} - \frac{|j_l|}{j_{c/2}^l} \quad (10)$$

$$j_{l,\alpha} = b_\alpha b_\beta j_\beta \quad (11)$$

Here  $\sigma_n$  is the electrical conductivity in the normal state. In this notation the critical surface defined by (5) corresponds to  $\sigma_{\text{eff}} = 2\sigma_n$  and parameters  $T_c$ ,  $B_{c2}$  and  $j_{c/2}$  are the intercepts of the critical surface with reference axes. Parameter  $\delta$  characterizes the width of a gradual kinetic transition from superconducting to normal state. In the limit  $\delta \rightarrow 0$  our scheme tends to the critical state model [Bean, 1962]. As  $\delta$  varies in the range 0.05–0.005, the values of  $T_c$  and  $B_{c2}(0)$  appear to be close to the related thermodynamic quantities (generally, these parameters may be redefined if needed).

There is no trace of thermal activation process in the experimentally approved HPSC constitutive law. An alternative model is statistic one. [Baixeras&Fournet, 1967].

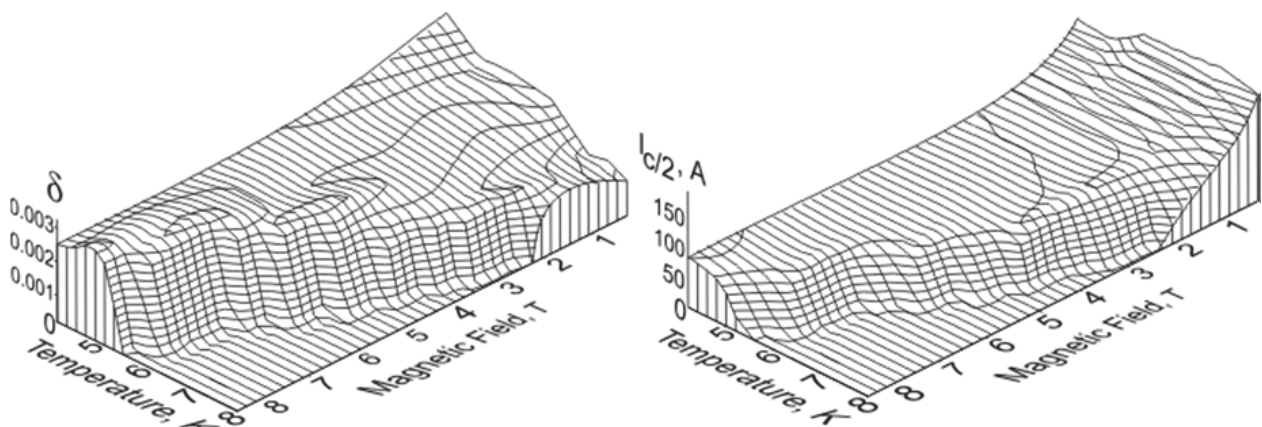


Fig. 3. These parameters weakly depends on temperature as well as on magnetic field.

It appeared that (1) described well transition of a model multilinked network consisting of superconducting elements if their critical temperatures had been normally distributed around certain mean value (Fig.4a) [Klimenko, 1983, 1985]. This model bears relation to “bulk inhomogeneous” superconductor such as monofilament wire. Another type of wires was current important in eighties. It was multifilament wire with broken filaments. This type needed another approach. We proposed regarding it as “longitudinally inhomogeneous” [Dorofeev et al., 1980].

$$V = R_m \int_0^I \frac{I - i_c}{\sigma \sqrt{2\pi}} \exp\left[-\frac{(I - i_c)^2}{2\sigma^2}\right] di_c \quad (12)$$

This carrying back makes sense due to far-reaching analogy between voltage-current curves of longitudinally inhomogeneous wires and modern HTSC. It would be absurd to look for any physical reasons of the analogy. Statistical reason seems more probable. This hypothesis helps discussing some features of HTSC, though, certainly, no analogy has evidential force.

A group of voltage-current curves according to (12) is presented at Fig.4b,c. In semi-logarithmic scale the curves are parabolas (Fig.4b), as it was shown and experimentally approved in [Dorofeev et al., 1980]. However, the SC community had preferred straightening curves by using logarithmic scale at both coordinates (Fig.4c). This transformation had given power behaviour to rather long parts of the curves. This explanation looks less naive than a model known as “logarithmic potential well” [Zeldov et al., 1990].

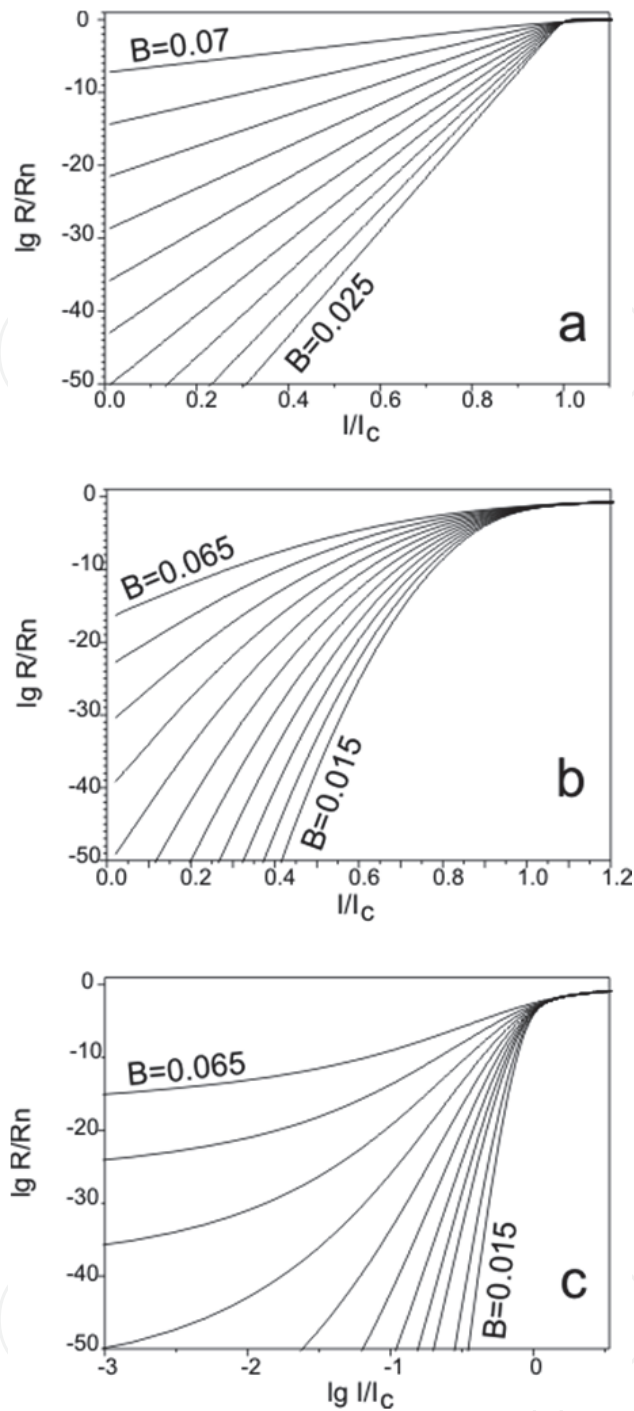


Fig. 4. Om-ampere curves of bulk inhomogeneous (a) and longitudinal inhomogeneous (b,c) superconductors.

An irreversible line is used to consider as one of the important characteristic of HTSC. It is assumed that this line separates voltage-current curves with positive and negative curvatures, the negative curvature considering as an evidence of the true superconducting condition. Fig.4c hints that irreversible line, perhaps, has no real sense. In fact, every curve changes its curvature from negative value to positive one at certain resistance level. The positive curvature itself arises due to stretching the current coordinate by logarithmic scale at low currents.

### 3. Electrodynamics equations

The electrodynamics of isotropic HPSC may be described in terms of the general quasistationary electrodynamics of a continuous media. In fact all the known HPSC are anisotropic. However, isotropic electrodynamics is ever considered as a necessary step [Klimenko et al., 2010].

$$\operatorname{rot}\mathbf{E} = -\frac{\partial\mathbf{B}}{\partial t} \quad (13)$$

$$\operatorname{div}\mathbf{B} = \quad (14)$$

$$\operatorname{rot}\mathbf{B} = \mu_0\mathbf{j} \quad (15)$$

Here  $\mathbf{E}$  and  $\mathbf{B}$  are the electric and magnetic fields, respectively,  $\mathbf{j}$  is the current density, and  $\mu_0$  is the magnetic constant. At a boundary of superconductor 1 and normal metal 2 the following components must be continuous

$$\mathbf{B}^{(1)} = \mathbf{B}^{(2)} - \mathbf{M}(B^{(2)}) \quad (16)$$

$$\mathbf{nE}^{(1)} = \mathbf{nE}^{(2)} \quad (17)$$

$$\mathbf{nj}^{(1)} = \mathbf{nj}^{(2)} \quad (18)$$

here  $\mathbf{n}$  is the unit vector normal to a boundary.  $\mathbf{M}$ -is magnetic moment of ideal type II superconductor. Ch. Bean [Bean, 1962] was the first, who had neglected this value. In fact, it is rather small, if  $\kappa = \frac{\lambda}{\xi} \gg 1$ :  $(M(B) = \frac{B_{c2}-B}{(2\kappa^2-1)\beta_A})$

Instead of electric and magnetic fields, it is more conveniently to use the scalar and vector potentials,

$$\mathbf{B} = \operatorname{rot}\mathbf{A} \quad (19)$$

$$\mathbf{E} = -\nabla\varphi - \frac{\partial\mathbf{A}}{\partial t} \quad (20)$$

In terms of potentials (19) and (20) the equations of electrodynamics are given by

$$\nabla^2 A_\alpha = \mu_0 \sigma_{\alpha\beta} \left( \nabla_\beta \varphi + \frac{\partial A_\beta}{\partial t} \right) \quad (21)$$

$$\nabla_\alpha \left( \sigma_{\alpha\beta} \left( \nabla_\beta \varphi + \frac{\partial A_\beta}{\partial t} \right) \right) = 0 \quad (22)$$

The potentials  $\varphi$  and  $\mathbf{A}$  should be continuous and satisfy boundary conditions (16–18).

Due to high sensitivity SC conductivity to temperature the electrodynamics equations must be supplemented by the heat transfer equation

$$C(T) \frac{\partial T}{\partial t} = \nabla_\alpha (\kappa_{\alpha\beta}(T) \nabla_\beta T) + G(T) \quad (23)$$

with Neumann boundary conditions. Here  $C(T)$  is the specific heat per unit volume,  $\kappa_{\alpha\beta}(T)$  is thermal conductivity, and the heat generation  $G(T)$  is determined as

$$G(T) = \mathbf{jE} \quad (24)$$

The constitutive law (6,9) permits to enclose the set of equations.

A package of computer codes was developed on the basis of Eq(21-24) for real geometry and heat exchange condition. It provides a possibility of stability and AC loss computation for arbitrary cycles of external magnetic field and current. The results will be soon published on behalf of the whole team.

#### 4. 2D voltage-current curves

The introduced above tensor conductivity is in contradiction with a widespread belief that current and electric field are collinear in isotropic superconductor:  $\mathbf{j} = j_c \frac{\mathbf{E}}{E}$ . [Carr, 1983].

W.J. Carr had supposed it as an intuitive generalization of Bean model. However the generalisation has appeared wrong. It is right only for the case of magnetic field perpendicular to current, as well as Bean model. Indeed moving vortices generate electric field in a plane normal to magnetic field. This field must be tilted to the current, if later does not lie in the plane.

$$\mathbf{E} = [\mathbf{B}\mathbf{v}] = \rho_t[\mathbf{j} - \mathbf{b}(\mathbf{j}\mathbf{b})] \quad (25)$$

The normal to current electric field component was called "satellite electric field" [Klimenko 2001a]. Fig.5 brings it clearly. It is significant that the tilt disappears, when the external magnetic field exceeds critical value, and the field components become independent. It may be the most convincing demonstration of electric field generating by vortices movement in superconductors.

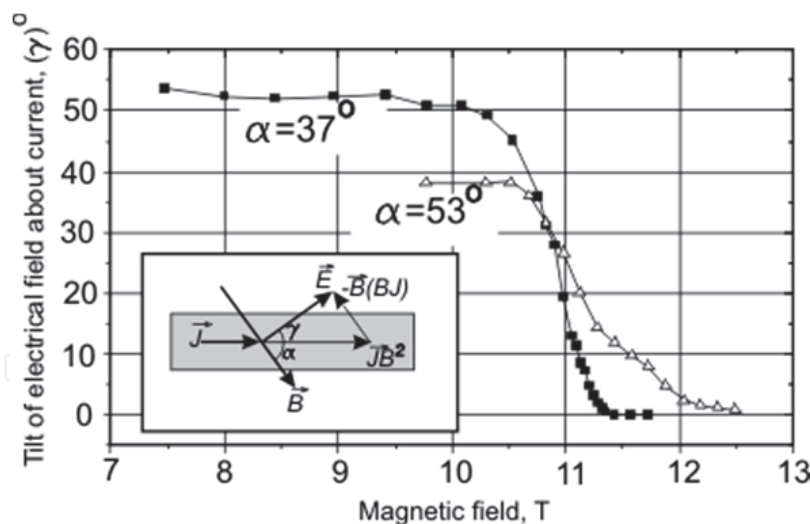


Fig. 5. The satellite electric field observation at 10  $\mu\text{m}$  Nb-Ti foil covered with 1  $\mu\text{m}$  layer of copper ( $\phi=37^\circ$ ) and -the same foil without copper layer ( $\phi=53^\circ$ ).

Another significant feature is quite large field interval ( $\sim 2\text{T}$ ) in which the tilt falls to zero. It is evidence of inhomogeneity of the superconductor. In all likelihood, the critical fields of elongated grains bodies and their borders are different. This assumption is supported with results of the similar experiment with the same foil samples cut at various angles to rolling direction. (Fig.6). One can see pikes in the transition interval. The current flows at angle to the superconducting borders and must to cross normal bodies generating transversal electric field.

## 5. Pinning anisotropy

There are no isotropic HPSC actually. Their electrodynamic is mainly of theoretical interest. Real anisotropic pinning brings to a wide variety of phenomena and will provide a lot of new “discoveries” if the proper electrodynamic is not developed in the nearest future.

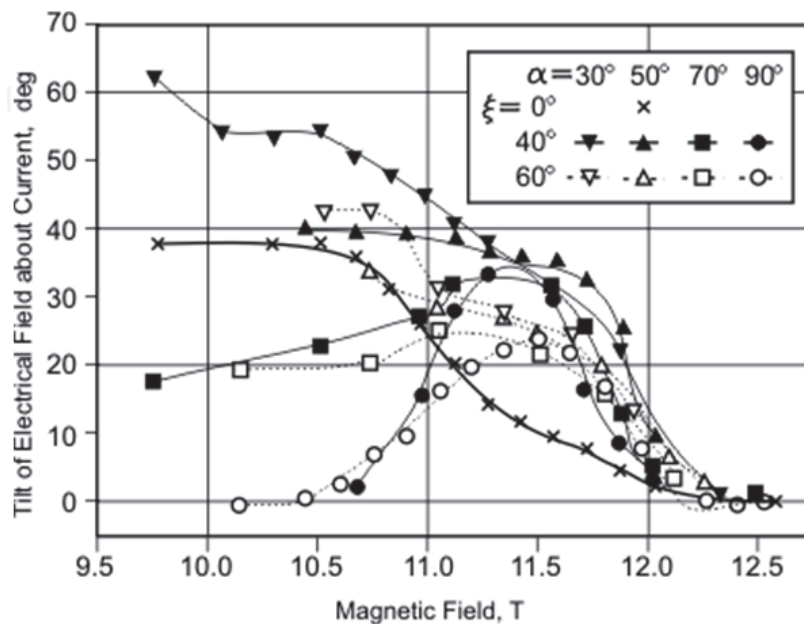


Fig. 6. The satellite electric field observation at the same foil samples cut at angle  $\xi$  to the rolling direction.

We cannot yet offer something being equivalent to the theory described in part 3. An approach [Klimenko et al., 1997] was developed in frames of critical state model. That time we used Critical Lorentz Force for critical state description. Critical Lorentz force (scalar) related to unit superconductor volume is a radius of certain closed surface (called “pinning surface”) in a space of Lorentz forces. Notice, subsequent reasoning always relates to unit superconducting volume. In the case of isotropic superconductor critical Lorentz force doesn’t depend on Lorentz force direction and the pinning surface is 3D sphere. In the case of anisotropic pinning the critical Lorentz force depends not only on Lorentz force direction but also on magnetic field direction. So the pinning surface must be constructed in 5D space: three components of magnetic field plus only two components of Lorentz force because the Lorentz force is always normal to magnetic field.

The following procedure was proposed as a simplest option of the pinning 5D-surface construction. It is well known that energy of pinned array of vortices is less than energy of free one. It means that the pinning array forms a potential well, which may be described with three parameters: height, width and steepness of a potential barrier. The height is an energy gain of pinned magnetic flux at rest. The width is a distance between nearby positions of the flux with the same energy gain. It is obvious that the width equals to the least of two mean values: distance between pinning centers or between vortices. The barrier steepness is a maximum derivative of the flux energy with respect to coordinate when the flux is displaced from the rest position. If shapes or distribution of pinning centers are anisotropic, the barrier parameters are described with tensors corresponding to certain ellipsoids which main diameters are aligned with the main directions of the pinning centers array.

Tensor U corresponds to the barrier height:

$$U = \begin{vmatrix} \frac{1}{U_x^2} & 0 & 0 \\ 0 & \frac{1}{U_y^2} & 0 \\ 0 & 0 & \frac{1}{U_z^2} \end{vmatrix} \quad (26)$$

The flux energy gain  $U_b$  at rest depends on magnetic field direction. It equals U-ellipsoid radius collinear to the magnetic field.

$$U_b^2 = (\mathbf{bUb})^{-1} \quad (27)$$

here  $\mathbf{b} = \frac{\mathbf{B}}{|\mathbf{B}|}$  is a unit vector in magnetic field direction.

Tensor L will help to calculate critical Lorentz force in direction  $l$ , which is  $F_{Ll}^c = \max(\frac{\partial u}{\partial l})$ ,

$$L = \begin{vmatrix} \frac{1}{l_{ex}^2} & 0 & 0 \\ 0 & \frac{1}{l_{ey}^2} & 0 \\ 0 & 0 & \frac{1}{l_{ez}^2} \end{vmatrix} \quad (28)$$

here  $l_{ei} = \frac{U}{\max(\frac{\partial u}{\partial l_i})}$ . This effective barrier half-width allows critical Lorentz force calculating:

$$F_L^c = \frac{U(B)}{l_e(f)} \quad (29)$$

$\mathbf{f} = \frac{\mathbf{F}_L}{|F_L|}$  is a unit vector in Lorentz force direction, and

$$l_e^2 = (\mathbf{fLf})^{-1} \quad (30)$$

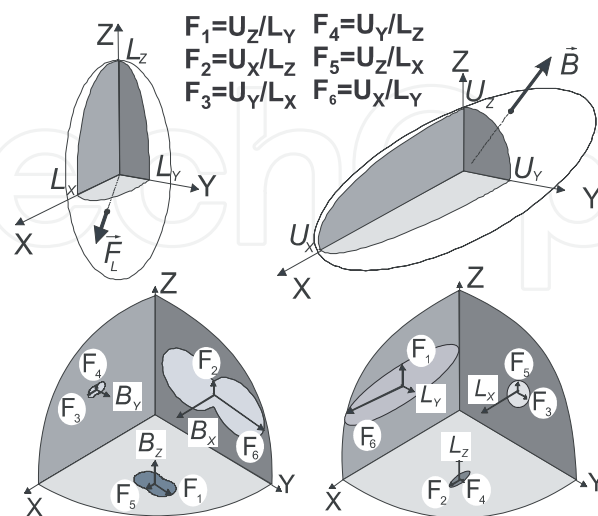


Fig. 7. The depth of potential well as well as the half-width of the potential barrier are described either with the symmetrical tensors of second valence or the ellipsoids corresponding to the tensors. The pinning surface main 2D cross sections are shown.

The effective half-width was assumed a geometrical parameter independent on  $U_b$ . Experimental data treatment must show, if the assumption was correct. The complete pinning surface may be constructed by division all radii of U-ellipsoid by L-ellipsoid radii in its cross section normal to the field directions. Fig.7 shows some 2D-cross-sections of the 5D pinning surface. Fig. 8. shows an example of 3D-cross section built for varying magnetic field directions.

The model doesn't allow getting all the six main diameters of the ellipsoids from critical Lorentz forces measurements. It is possible to write six values:

$$F_{Lij}^c = \frac{U_i}{J_{eff}^j}, \quad i \neq j \quad (31)$$

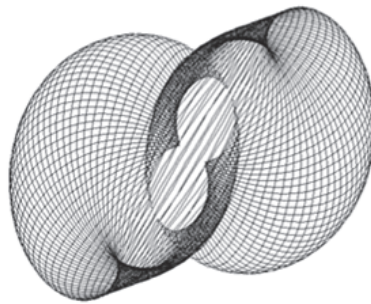


Fig. 8. 3D- cross section of a pinning surface. (U- ellipsoid main radii are related as 1:2:3, L- ellipsoid ones - as 1:2;4. Magnetic fields vectors are laying in the U-central plane with radii related as 1:3).

It is easy to see that  $F_{L13}^c F_{L21}^c F_{L32}^c = F_{L12}^c F_{L23}^c F_{L31}^c$ . Thus, only five of them are independent on one another.

We have studied a large series of samples made from cold deformed Nb-Ti foil. They were cut at various angles to rolling direction and tested in magnetic fields tilted at various angles both to the sample plane and current direction. Fig.9 shows the main radii of the ellipsoids, the barrier half-width  $L_y$  normal to the foil plane being accepted as unity. The pinning centers density in this direction was maximum, and the half-width didn't change while magnetic field increased in contrary with  $L_x$  aligned to the rolling direction.

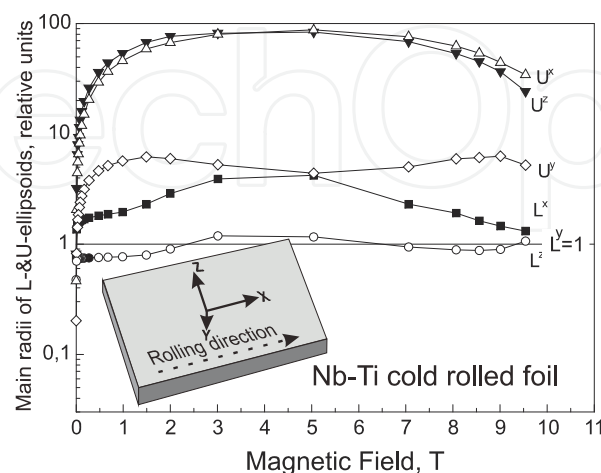


Fig. 9. The main radii of L- and U- ellipsoids of the cold rolled Nb-Ti 10  $\mu$  foil. The data are extracted from a set of experiments with various orientations of magnetic fields and currents.

The degree of the foil anisotropy is seen from Figs.10 and 12. It allows estimating of agreement between experimental data and model predictions.

There are two causes of transverse electric field origin. The above-mentioned satellite field arises due to movement of vortices tilted to current direction. Another one is known as guided vortices motion [Niessen&Weijnsfeld, 1969]. It arises due to vortices movement at an angle to Lorentz force direction. Fig. 11a explains this phenomenon. Due to the special shape of a cross section of the pinning surface normal to the magnetic field, a certain projection of the Lorentz force vector pierces the pinning surface in point 'd', whereas the vector itself does not reach point 'c' at the surface. So the magnetic flux moves in the projection direction. Fig.11b compares the prediction with our experimental data.

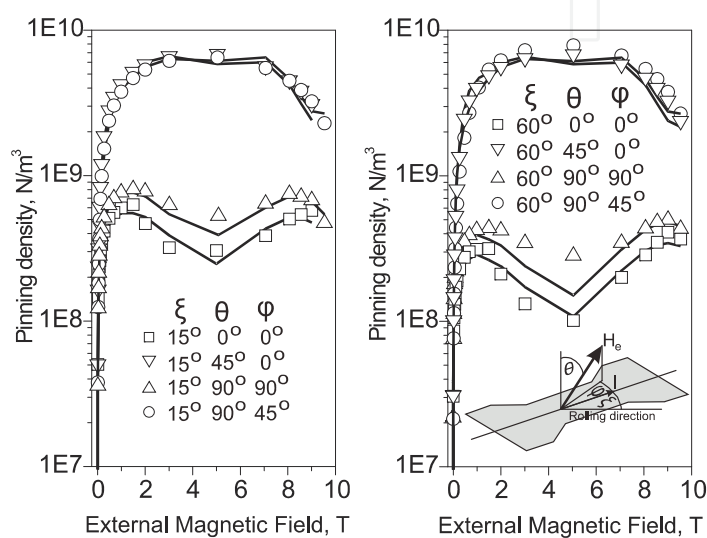


Fig. 10. A comparison of the experimental data on pinning density with predictions (solid curves) calculated with the main radii of L- and U- ellipsoids. The dependence of the pinning anisotropy on both the magnetic field and Lorentz force directions can be seen.

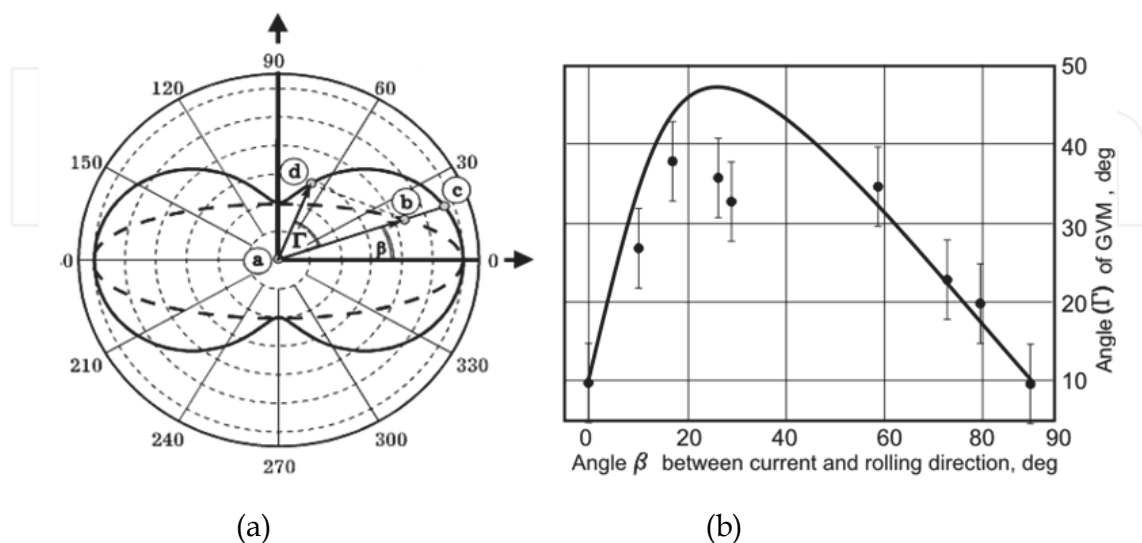


Fig. 11. A scheme of guiding vortices motion arising (left) and comparison of experimental points and predicted curve (right) obtained by magneto-optical method in low magnetic field.

A problem of critical current in longitudinal magnetic field was very exciting for a long time due to nontrivial process of vortices reconnecting. There were tested four foil samples in magnetic field aligned to current direction with accuracy better than  $0.2^\circ$ . The samples were cut at different angles  $\xi$  to the rolling direction. Fig.13 shows results of foil samples testing compared with model calculations made on the following assumptions: a. The vortices reconnection is free at pinning centers, b. The vortices array breaks virtually up into longitudinal and transverse ones moving in opposite directions, c. pinning centers number is sufficient for independent pinning of both virtual arrays. The semiquantitative agreement is obvious. The model predicts correctly nontrivial dependence of longitudinal critical currents on pinning.

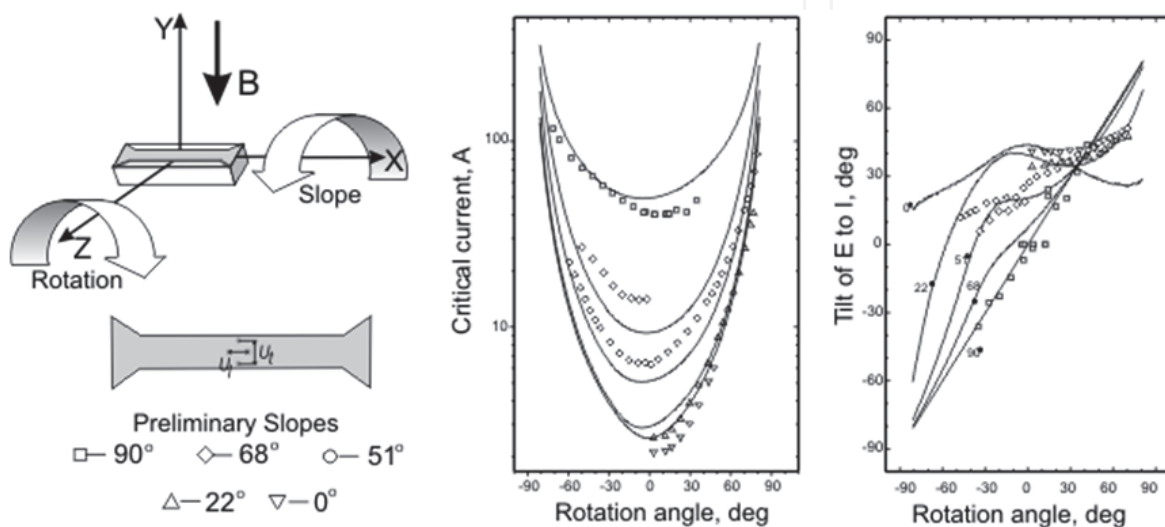


Fig. 12. Results of studying critical currents and tilts of electrical field to current directions in dependence on preliminary slopes and rotation angles.

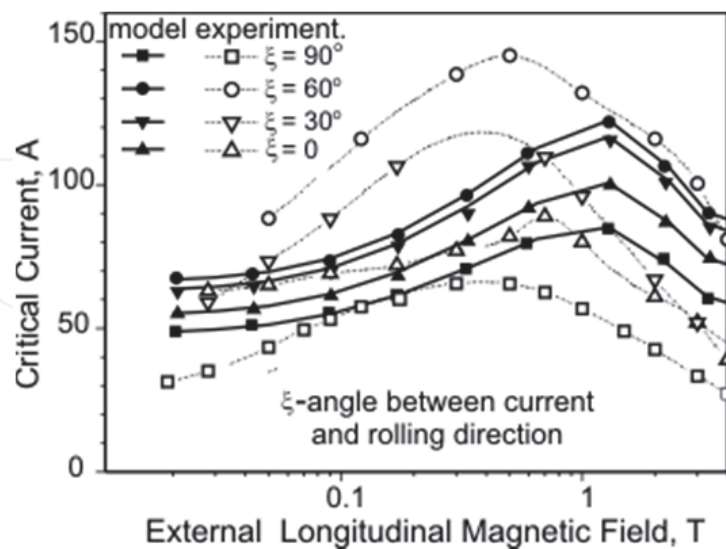


Fig. 13. The critical currents in the longitudinal magnetic fields. The experimental values obtained with the samples (1.3 mm width) cut from a piece of Nb-Ti  $10 \mu\text{m}$  foil at various tilts to the rolling direction are compared with predictions (curves) calculated with the main radii of L- and U- ellipsoids (Fig.9)

The foil anisotropy arises due to the rolling process. The wire drawing process has certain features in common with rolling. It also forms the anisotropic structure. Significant difference in critical current values for axial and azimuth currents is well known [Jungst, 1977]. It appeared that significant pinning anisotropy existed in a wire cross section [Klimenko et al., 2001b]. It was found out on trials of a Nb-Ti wire 0.26 mm in diameter with cross section reduced by grinding into segment shape (segment height was 0.21 of the wire diameter).

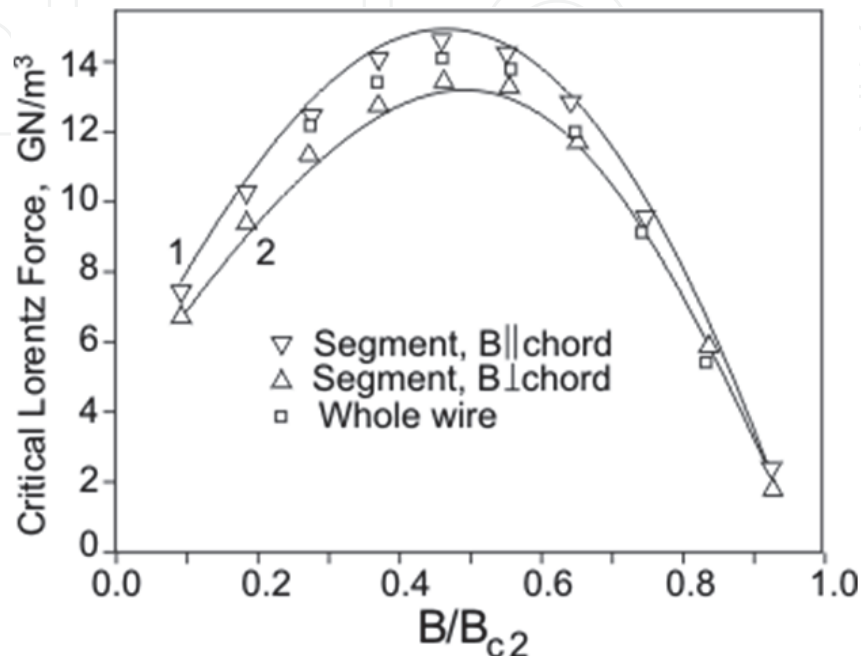


Fig. 13. Critical Lorentz Force anisotropy in Nb-Ti wire cross section. 1. The critical value for azimuthally aligned vortices, 2. The critical value for radial aligned vortices.

Maximum and minimum critical Lorentz Forces (curves 1 and 2 at Fig.13) were derived from results of segment tests in magnetic fields of orthogonal directions. The anisotropy affects the wire critical current and the magnetic moment. Figs.14 and 15 show these effects, the foil anisotropy parameters being used for the calculations to make the effects more pronounced. The results differ in dependence on prevalence of radial or azimuth pinning.

The anisotropy affects critical currents in low magnetic field, where azimuth component of the current self field becomes dominant (Fig.14), as it is seen from current distributions shown at the left pictures. When the azimuth aligned vortices pinning is higher than one of radial vortices the critical current rises steeply up as the field decreases (curve 2 at Fig.14). The Nb-Ti wire demonstrates just this type of  $I_c(B)$  curve. A material with opposite ratio of pinning forces would show a plateau in this field region (curve 1).

There is a large range of magnetic fields where critical currents don't depend on the type of anisotropy. Current distributions in this range are similar (right pictures of Fig.14). This independence allowed the constitutive law (part 2 of this paper) deducing under the assumption that the averaged current density had a definite physical meaning (part 6 of the paper).

The type of anisotropy influences on the wire magnetic moment in the whole range of magnetic fields due to difference in distances of current density maxima from the cross section symmetry lines (Fig 15).

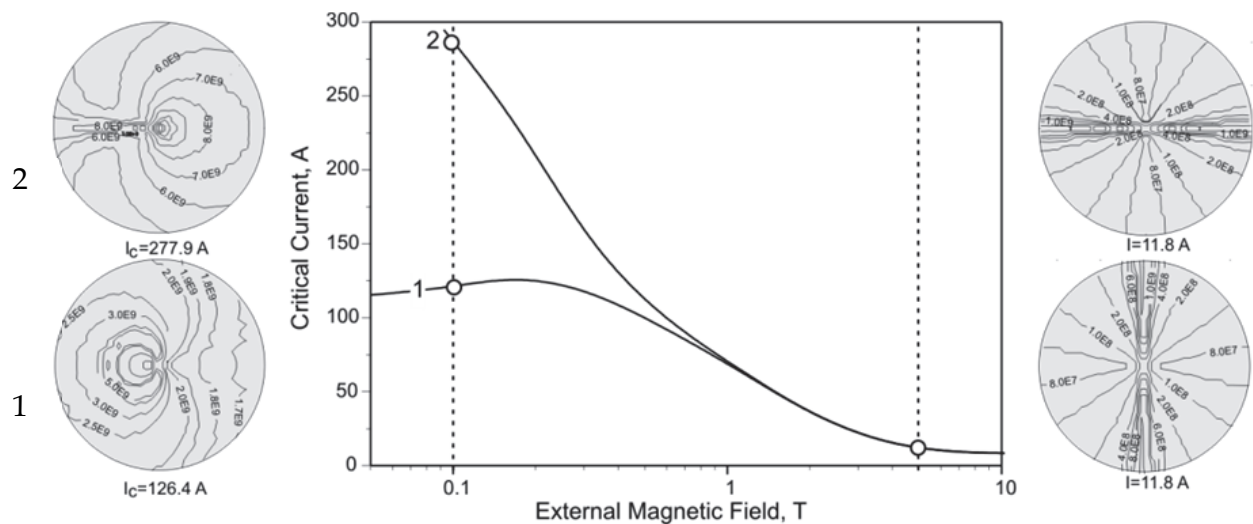


Fig. 14. Comparison of field dependences of the critical current of wires on the type of anisotropy. 1. Pinning of radial aligned vortices prevails. 2. pinning of azimuth aligned vortices prevails. Current density distributions in low and high magnetic fields are shown on left and right sides of the picture.

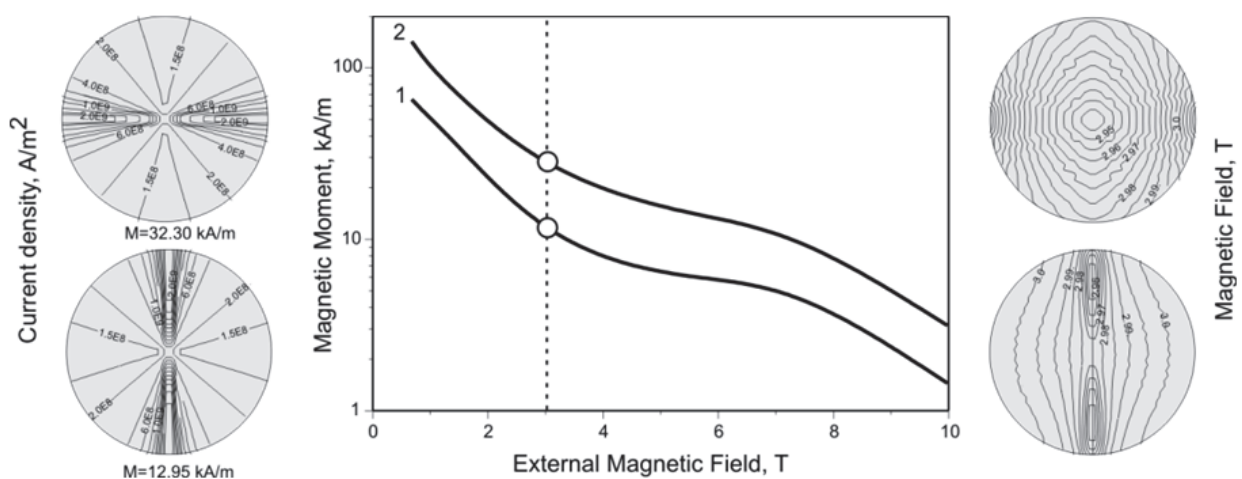


Fig. 15. Comparison of field dependences of the magnetic moments of wires on the type of anisotropy. 1. Pinning of radial aligned vortices prevails. 2. Pinning of azimuth aligned vortices prevails. Current density and magnetic field distributions are shown on left and right sides of the picture.

## 6. Self-consistent distributions of magnetic field and current density

The most of important problems of applied superconductivity, such as conductor stability, AC loss, winding quench, require nonsteady equations solving. There is, may be, only one situation which needs steady state analyzing. That is testing of a conductor, namely voltage-current curve registration. There is a crafty trap in this seemingly simplest procedure. The point is that this procedure gives an integral result that is dependence of the curves on external magnetic field or, less appropriately, dependence of critical current on the external magnetic field ( $I_c(H_e)$ ). This result is sufficient for a winding designer. A material researcher

needs differential result that is dependence of critical current density on internal magnetic field ( $j_c(B)$ ). It is considered usually that

$$j_c(\mu_0 H_e) = \frac{I_c(H_e)}{S} \quad (32)$$

Firstly, it is not trivial because current distribution is not homogeneous in conductor cross section due to current self field. There was shown [Klimenko&Kon, 1977] that in high fields

$$I_c(H_e) = j_c(\mu_0 H_e) \pi r_0^2 \left( 1 - 0.031 \frac{j_c(\mu_0 H_e) r_0}{H_e} \right) \quad (33)$$

here  $r_0$  - wire radius,  $j_c(B) \sim B^{-0.5}$  was assumed. Taken from the same paper Fig.16 shows that (32) may not be used in low external fields due to the current self field becomes more than the external field. An example of habitual mistake [Kim et al., 1963]: the dependence

$$j_c(B) = \frac{\alpha_c}{B+B_0} \quad (34)$$

by no means follows from more or less acceptable approximation :  $I_c(B_e) = \frac{C}{B_e+B_0}$

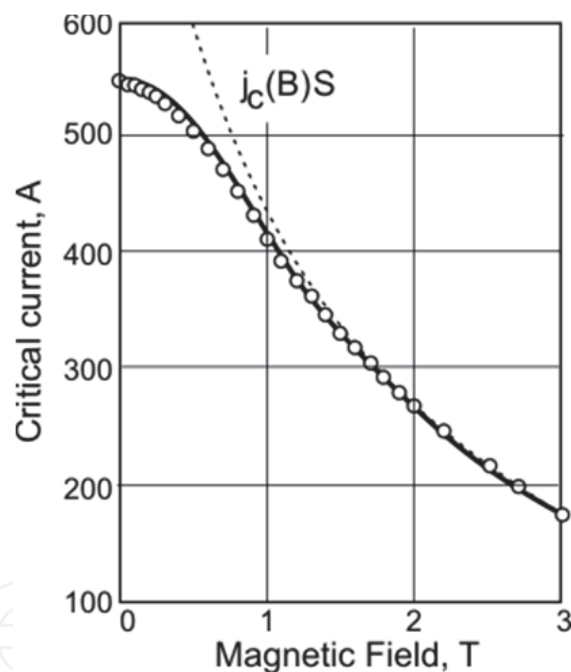


Fig. 16. Critical current dependence on external magnetic field calculated and measured for the case wire with Nb-Ti core 0.22 mm in diameter (Critical current density was assumed  $1.06 \cdot 10^{10} B^{-0.5}$  A/m<sup>2</sup>)

If the constitutive law is known, the self-consistent distributions of current density and inner magnetic field can be found by iterations for any external magnetic and electric fields. In the case of anisotropic pinning results of the solution seem to be unexpected. Fig.17 shows calculated critical currents of a tape 4 mm wide ( $a$ ) and 2  $\mu\text{m}$  thick ( $b$ ) for two anisotropy directions. The constitutive law was used in the form (1). It is seen that non-monotone run of the current curves is a macroscopic effect that follows from quite monotone critical current density falling with magnetic field rising.

The critical current corresponding to zero external magnetic field is the presently accepted standard of HTSC conductor evaluating. The insufficient information is not a main drawback of the standard. Sometimes it provokes false conclusions. Fig.18 suggests that HTSC layer thickness increasing uses to spoil the material properties; in fact the current density goes down due to current self field increasing.

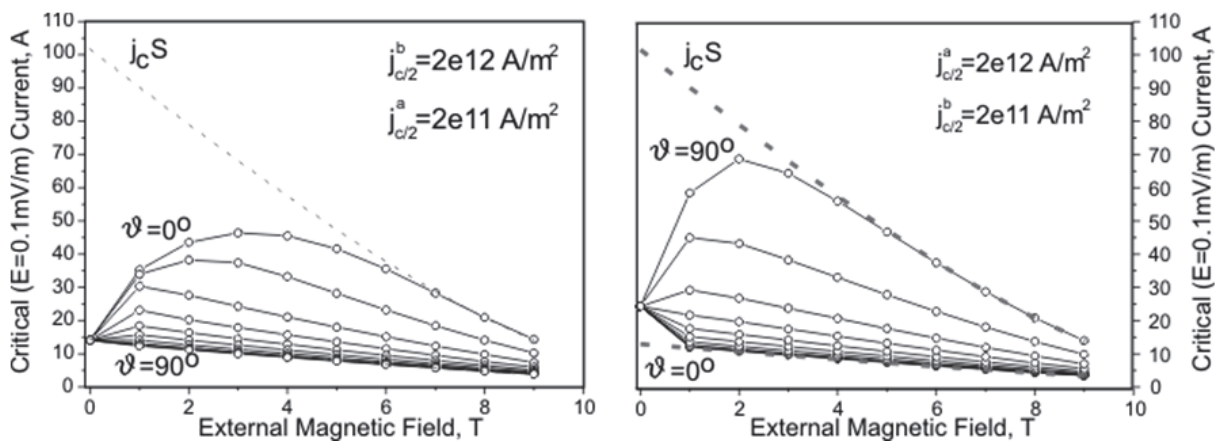


Fig. 17. Calculated  $I_c(B)$  curves depending on magnetic field tilt ( $\psi$ ) in respect to the normal to the tape surface for the cases when maximum critical Lorentz force direction aligns to the tape width (left) and to the thickness (right).

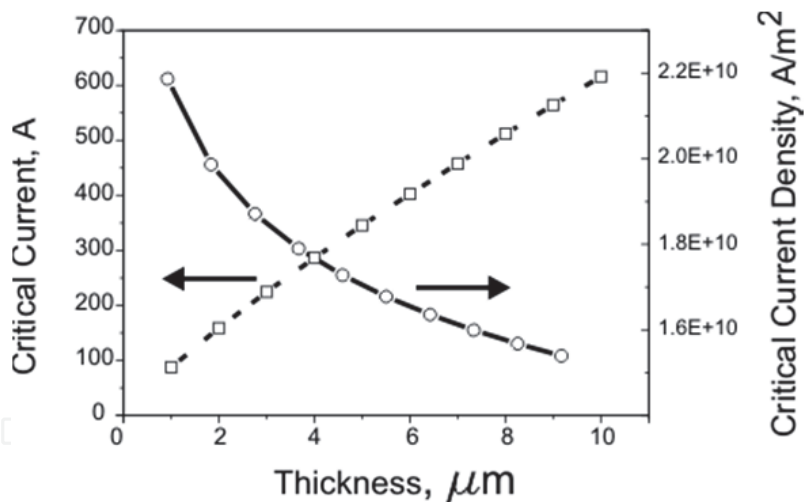


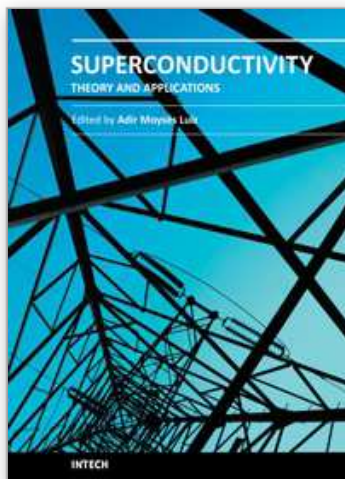
Fig. 18. Calculated dependence of critical current and averaged critical current density on the HTSC layer thickness.

## 7. Conclusion

There are countless numbers of complete phenomena and characteristics of HPSC discovered during last half century and last quarter in particular. We hope that the completeness is not inherent property of the HPSC but it is consequence of superposition of several quite simple features: nonlinear constitutive law, inhomogeneity, various types of anisotropy, self consistent distributions of magnetic field and current density and may be something else.

## 8. References

- Anderson P. W., (1962). Theory of Flux Creep in Hard Superconductors, *Phys. Rev. Lett.* 9, pp.309-311
- Baixeras J. and Fournet G., J. (1967). Pertes par déplacement de vortex dans un supraconducteur de type II non idéal *Phys. Chem. Solids* 28, pp.1541-1545
- Bean C.P. (1964), Magnetization of High-Field Superconductors, *Rev. Mod. Phys.* 36, 31-39
- Carr W.J. (1983) *AC Loss and Macroscopic Theory of Superconductors*, Gordon & Beach, ISBN 0-677-05700-8, London, New York, Paris.
- Dorofeev G. L., Imenitov A. B., and Klimenko E. Yu., (1980) Voltage-current characteristics of type III superconductors, *Cryogenics* 20, 307-310
- Dorofeev G. L., Imenitov A. B., and Klimenko E. Yu., (1978), Voltage-current curves of deformed SC wires of III type *Preprint No. 2987*, IAÉ (Inst. of Atomic Energy, Moscow)
- Jungst K.-P., (1975), Anisotropy of pinning forces in NbTi, *IEEE Transaction on Magnetics*, v.MAG-11, N2, 340-343
- Kim Y.B., Hempstead C.F., Strnad A.R., (1965), Flux-Flow Resistance in Type-II Superconductors, *Phys. Rev.*, v.139, N4A, A1163-A1172
- Klimenko E. Yu. and Kon V. G., (1977), On critical state of real shape superconducting samples in low magnetic field., in « Superconductivity »: *Proceedings of Conference on Technical Applications of Superconductivity*, Alushta-75 Atomizdat, Vol. 4, pp. 114-121
- Klimenko E. Yu. and Trenin A. E., (1983), Numerical calculation of temperature dependent Superconducting Transition in inhomogeneous Superconductor, *Cryogenics* 23, 527-530
- Klimenko E. Yu. and Trenin A. E., (1985), Applicability of the Normal distribution for calculation voltage-current characteristics of superconductors *Cryogenics* 25, pp. 27-28
- Klimenko E. Yu., Shavkin S. V., and Volkov P. V., (1997), Anisotropic Pinning in macroscopic electrodynamics of superconductors *JETP* 85, pp. 573-587
- Klimenko E. Yu., Shavkin S. V., and Volkov P. V., (2001), Manifestation of Macroscopic Nonuniformities in Superconductors with Strong Pinning in the dependences of the transverse Current-Voltage Curves on the magnetic Field near  $H_{c2}$ . *Phys. Met. Metallogr.* 92, pp. 552-556
- Klimenko E. Yu., Novikov M. S., and Dolgushin A. N., (2001), Anisotropy of Pinning in the Cross Section of a Superconducting Wire. *Phys. Met. Metallogr.* 92, pp. 219-224.
- Klimenko E. Yu., Imenitov A.B., Shavkin S. V., and Volkov P. V., (2005), Resistance-Current Curves of High Pinning Superconductors, *JETP* 100, n.1, pp. 50-65
- Klimenko E. Yu., Chechetkin V.R., Khayrutdinov R.R., Solodovnikov S.G., (2010), Electrodynamic of multifilament superconductors, *Cryogenics* 50, pp. 359-365.
- Ketterson J.B. & Song S.N. (1999). *Superconductivity*, CUP, ISBN 0-521-56295-3, UK Niessen A.K., Weijzenfeld C.H., (1969), Anisotropic Pinning and guided Motion of Vortices in Type II Superconductors, *J. Appl. Phys.*, 40, pp.384-393
- E. Zeldov, N. M. Amer, G. Koren, et al., (1990), Flux Creep Characteristics in High-Temperature Superconductors *Appl. Phys. Lett.* 56, pp. 680-682, ISSN: 0003-6951



## **Superconductivity - Theory and Applications**

Edited by Dr. Adir Luiz

ISBN 978-953-307-151-0

Hard cover, 346 pages

**Publisher** InTech

**Published online** 18, July, 2011

**Published in print edition** July, 2011

Superconductivity was discovered in 1911 by Kamerlingh Onnes. Since the discovery of an oxide superconductor with critical temperature ( $T_c$ ) approximately equal to 35 K (by Bednorz and Müller 1986), there are a great number of laboratories all over the world involved in research of superconductors with high  $T_c$  values, the so-called “High- $T_c$  superconductors”. This book contains 15 chapters reporting about interesting research about theoretical and experimental aspects of superconductivity. You will find here a great number of works about theories and properties of High- $T_c$  superconductors (materials with  $T_c > 30$  K). In a few chapters there are also discussions concerning low- $T_c$  superconductors ( $T_c < 30$  K). This book will certainly encourage further experimental and theoretical research in new theories and new superconducting materials.

### **How to reference**

In order to correctly reference this scholarly work, feel free to copy and paste the following:

Evgeny Klimenko (2011). Electrodynamics of High Pinning Superconductors, Superconductivity - Theory and Applications, Dr. Adir Luiz (Ed.), ISBN: 978-953-307-151-0, InTech, Available from:  
<http://www.intechopen.com/books/superconductivity-theory-and-applications/electrodynamics-of-high-pinning-superconductors>

**INTECH**  
open science | open minds

### **InTech Europe**

University Campus STeP Ri  
Slavka Krautzeka 83/A  
51000 Rijeka, Croatia  
Phone: +385 (51) 770 447  
Fax: +385 (51) 686 166  
[www.intechopen.com](http://www.intechopen.com)

### **InTech China**

Unit 405, Office Block, Hotel Equatorial Shanghai  
No.65, Yan An Road (West), Shanghai, 200040, China  
中国上海市延安西路65号上海国际贵都大饭店办公楼405单元  
Phone: +86-21-62489820  
Fax: +86-21-62489821

© 2011 The Author(s). Licensee IntechOpen. This chapter is distributed under the terms of the [Creative Commons Attribution-NonCommercial-ShareAlike-3.0 License](#), which permits use, distribution and reproduction for non-commercial purposes, provided the original is properly cited and derivative works building on this content are distributed under the same license.

IntechOpen

IntechOpen